Electronics and Electrical Engineering

https://www.aimspress.com/journal/ElectrEng

AIMS Electronics and Electrical Engineering, 8(2): 237–254.
DOI: 10.3934/electreng.2024011
Received: 16 March 2024
Revised: 23 April 2024
Accepted: 30 April 2024
Published: 10 May 2024

Research article

Collision detection and external force estimation for robot manipulators using a composite momentum observer

Benaoumeur Ibari*, Mourad Hebali, Baghdadi Rezali and Menaouer Bennaoum

Department of Electrotechnical, University of Mustapha Stambouli Mascara, Mascara, 29000, Algeria

* **Correspondence:** Email: ibari_b@univ-mascara.dz.

Abstract: The collision detection and estimation of external forces for robot manipulators are essential to ensure compliance and safety in the interaction between the robot and the environment or humans. The focus of this paper was to design a hybrid approach for collision detection between robots and their environment, and further to estimate external forces acting on a robot manipulator without the need for additional sensors. The current collision detection methods using observers are still suffering from the problem of an unavoidable trade-off between the estimation sensitivity and the reduction of the peaking value at the initial time. To satisfy both robustness and avoid peaking phenomenon at the initial time, a composite observer was designed, consisting of both a momentum observer and an extended state observer. The first observer provides high-precision tracking, while the second one reduces the peak value at the start. Through their complementary roles, the composite observer achieves improved performance in terms of sensitivity and reducing the peaking value. Simulation results, conducted using a 2-degree-of-freedom (2-DOF) robot manipulator, attest to the efficacy of the proposed approach.

Keywords: robot manipulator; collision detection; force estimation; momentum observer

1. Introduction

In robotics applications, a robot manipulator typically operates in dynamic, unstructured environments and also interacts physically with human operators, which threatens the safety of humans and equipment. The need for improved collision detection methods in robotics, particularly in applications involving human-robot interaction, stems from several crucial factors: safety, efficiency, precision, and regulatory compliance. Increasing the admittance at the interaction interface between the robot and the user (e.g., diminishing the effective inertia and damping applied to external forces) offers several benefits, including enhanced safety by minimizing collision forces and facilitating collaborative manipulation with humans [1]. Therefore, the first and most important requirement when designing

a collaborative robotic cell is to ensure the safety of the human operator [2, 3]. Thus, fast and reliable contact or collision detection is crucial to perform the required reaction. The regulatory frameworks play a very important role in developing safe and efficient robot arm systems for real-world applications. In [4], the objective was to provide a theoretical framework for designing safety-related controllers in robotics systems. This framework ensures safety and efficiency in real-world applications, including human-robot collaboration in industrial setups.

Current collision detection methods can be divided into two categories, model-based methods and model-free methods. In model-free methods, there are also two subcategories, the first is based on additional external sensors attached to the manipulator for detecting collisions and calculating the magnitudes of impact forces, such as skin sensors [5–8], additional vision [9], and accelerometer sensors [10, 11]. In [12], a collision detection method was developed specifically for high payload applications. This approach utilized a force/torque sensor at the end effector and motor current measurements to ensure redundancy. The technique integrated a bandpass filter with differentiation, forming an effective foundation for collision detection by minimizing the effects of low-frequency signals and high-frequency noise. Experimental validation confirmed the effectiveness of the results. Therefore, the effectiveness of the method relies on the accuracy of the sensors used. However, this technology could increase the manufacturing cost of the robots and complicate their structure. The second subcategory is based on artificial intelligence techniques [13–19]. These techniques are based on training the robot through appropriate excitation collisions to recognize real collisions during robot operation, and this should include sensor data recorded during various collision scenarios. However, obtaining a detection model and improving its detection accuracy requires a substantial amount of data, which can be a hindrance to the practical application of these techniques.

Model-based methods rely on the robot's dynamic model, therefore, they have been more successful than model-free methods when considering both cost and practical application aspects. In traditional model-based approaches [20,21], collision detection relies on an inverse dynamic model (IDM). This is achieved by monitoring the residual signal, which quantifies the difference between the measured joint torque and the estimated joint torque. This method necessitates the calculation of joint acceleration, achieved by taking the derivative of the velocity signal, thereby introducing additional noise into the measurement. In [22], an alternative approach was presented based on a velocity observer, where a simplified observer was used to estimate the velocity signal and subsequently transformed this model into a perturbation observer for determining the joint's unknown external torque. The dynamics of this observer necessitated the use of an inverse inertia matrix, leading to an increase in computational cost. In [23], a disturbance Kalman filter (DKF) was proposed, which possessed disturbance immunity but exhibits reduced sensitivity primarily because of limited model accuracy. In [24], an innovative observer was designed, based on joint momentum dynamics, which operated independently of the inverse inertia matrix. Of the recent mentioned methods, there is a general consensus that the momentum observer-based approach stands out as the most accurate, dependable, and cost-effective. However, it does produce an unwanted peak during the initial period, which may potentially trigger a false contact detection alert. The GMO, or generalized momentum observer, functions as a first-order filter, taking the collision as an input signal and producing a momentum residual as an output signal, as depicted in [25]. Several studies have suggested enhancements to further refine the performance of the momentum observer. Such as in [26], the sliding mode technique was combined with a momentum observer to ensure the finite-time convergence of the estimated external force to the actual external

force. In [27], the authors introduced a novel sliding mode momentum observer (NSOMO) designed to eliminate the chattering phenomenon. This was achieved through the implementation of a new reaching law. In [28], a collision detection algorithm was developed specifically for industrial robot force/position hybrid control scenarios, addressing safety concerns. This algorithm incorporated a collision detection model based on dynamics and utilized a continuous friction model to enhance joint friction compensation, proving effective in experimental settings. In [29], the paper proposed an adaptive collision threshold based on the robot's speed and acceleration using a fuzzy logic system, enhancing collision detection in robot manipulators. This method aimed to improve performance by adjusting the threshold value dynamically, based on real-time variations in the robot's dynamics.

1.1. Relevant work

To reduce the peak phenomenon associated with the momentum observer, an alternative dynamic configuration was introduced [30], leveraging the extended state of the momentum observer as detailed in [31]. This modification transformed it into a second-order filter with a defined bandwidth that impacts both the sensitivity of force estimation and the occurrence of peak phenomena within the observer. However, a limitation of this observer lies in its inability to strike a balance between sensitivity and reducing peak values. In response to the challenge of an inherent trade-off between collision sensitivity and peak value reduction in the initial time, a solution was proposed by [32]. The authors designed a compromise approach that incorporated nonlinear functions into the state observer design. This approach, known as the nonlinear generalized momentum observer (NGMO), achieved the balance by providing the necessary bandwidth for collision detection observation. While enhancing the extended momentum observer through the incorporation of nonlinear functions can lead to improved performance, this approach comes with certain drawbacks. Most important, the selection of these nonlinear functions is primarily empirical in nature, and it presents particular challenges when it comes to proving the observer's stability due to the inherent complexity of these nonlinear functions.

Motivated by the issues discussed previously, this paper presents a hybrid approach to address the inherent trade-off between collision sensitivity and peak value reduction. Collaborative construction of a composite observer involves two key components: the momentum observer and the extended state observer. The extended state observer is initially employed with a suitable bandwidth to eliminate peak phenomena during the initial phase. Once the peaks are successfully mitigated, the system switches to the momentum observer with suitable gain to achieve high sensitivity in force estimation. These two observers operate collaboratively, each providing distinct benefits to enhance both peak value reduction and estimation sensitivity.

The paper is organized as follows. Section 2 briefly presents the robot dynamic model and preliminaries. In Section 3, we introduce the proposed method, known as the composite momentum observers, for the estimation of external forces. In Section 4, the obtained results are compared to the state-of-the-art simulation. Finally, Section 5 summarizes the work.

2. Robot modelling

The behavior of an n-degree-of–freedom robot manipulator can be represented by the following dynamic equation.

$$M(q)\ddot{q} + C(q,\dot{q})\dot{q} + G(q) = \tau + \tau_{ext} \tag{2.1}$$

where $q, \dot{q}$ and $\ddot{q} \in \mathbb{R}^{n\times 1}$ are the vectors of the joint position, velocity, and acceleration, respectively. $M(q) \in \mathbb{R}^{n\times n}$ is the inertia matrix, which characterizes the distribution of masses and moments of inertia within the robot system, $C(q,\dot{q}) \in \mathbb{R}^{n\times n}$ is the Coriolis, and centrifugal forces matrix that relates the joint velocities and accelerations of the system to the forces and torques exerted on the system. It takes into account the nonlinear effects resulting from the relative motion between different parts of the robot. $G(q) \in \mathbb{R}^{n\times 1}$ is the gravity vector, $\tau \in \mathbb{R}^{n\times 1}$ is the internal torque provided by the robot's actuators and, $\tau_{ext} \in \mathbb{R}^{n\times 1}$ represent the external torque/force vector resulting from an environment or human collision.

Lemma 1. *[33] The matrix $M(q) - 2C(q,\dot{q})$ is skew-symmetry, and so it follows that*

$$\dot{M}(q) = C(q,\dot{q}) + C^T(q,\dot{q}) \tag{2.2}$$

where C^T is the matrix transpose of C.

3. Observer design

3.1. Generalized momentum observer

When a collision occurs, it results in a change in the momentum of the system. This change can be estimated by the observer. The motivation behind the monitoring method, which relies on the generalized momentum observer as presented in [34, 35], was driven by the goal of not the necessity for inverting the robot's inertia matrix. This approach aims to decouple estimation results and eliminate the requirement for estimating joint accelerations. The generalized momentum of the robot is defined as follows

$$p = M(q)\dot{q} \tag{3.1}$$

The time derivative of (3.1) can be written as

$$\dot{p} = \dot{M}(q)\dot{q} + M(q)\ddot{q} \tag{3.2}$$

Using (2.1) and (2.2), (3.2) can be expressed as follows

$$\dot{p} = \tau + \tau_{ext} + C^T(q,\dot{q})\dot{q} - G(q) \tag{3.3}$$

To estimate the unknown quantity τ_{ext} resulting from a collision, the momentum observer dynamics are defined as follows

$$\begin{cases} \dot{\hat{p}} = \tau + C^T(q,\dot{q})\dot{q} - G(q) + r \\ \dot{r} = L(\dot{p} - \dot{\hat{p}}) \end{cases} \tag{3.4}$$

where $r \in \mathbb{R}^{n\times 1}$ is the residual vector, which represents external force estimation, $\hat{p}$ is the estimate value of momentum p, and $L = diag\{l_i\} > 0$ is a gain matrix of the observer.

The output of the momentum observer, denoted as $r(t)$, can be described by the following equation

$$r(t) = L(p(t) - \int_0^t (\tau + \hat{C}^T(q,\dot{q})\dot{q} - \hat{G}(q) + r)dv + p(0)) \tag{3.5}$$

Using a Laplace transformation on both sides of (3.4) gives

$$sr(s) = L(\tau_{ext} - r(s)) \tag{3.6}$$

thus

$$\frac{r(s)}{\tau_{ext}} = \frac{L}{L+s} \tag{3.7}$$

From (3.7), in the absence of a collision, the observer r converges to zero following the exponential rule. However, when a collision occurs, r converges to τ_{ext}. The collision algorithm is inherently first-order, as it only involves a single adjustable parameter. Consequently, achieving a balance between accuracy and speed becomes challenging. When the observer gain is increased, it results in significant peak values, and a reduction in gain leads to a loss in estimation sensitivity.

3.2. Extended state momentum observer

As an innovative observer design, the extended state observer was initially introduced by [36]. The core concept behind this observer is the utilization of an augmented state vector for unknown nonlinear function estimation. From (3.3), we construct the first-order state-space equation based on the generalized momentum as follows

$$\begin{cases} x_1 = p \\ \dot{x}_1 = \tau + \tau_{ext} + C^T(q,\dot{q})\dot{q} - G(q) \\ y = x_1 \end{cases} \tag{3.8}$$

If τ_{ext} is considered an extended state of (3.8), the second-order state-space can be written as

$$\begin{cases} x_1 = p \\ \dot{x}_1 = x_2 + \tau + C^T(q,\dot{q})\dot{q} - G(q) \\ \dot{x}_2 = \varphi(t) \\ y = x_1 \end{cases} \tag{3.9}$$

where x_2 is the extended state, and $\phi(t)$ is an unknown bounded function such that $\phi(t) \leq \epsilon$, (ϵ positive value).
The extended state observer is designed according to (3.9) as

$$\begin{cases} \dot{z}_1 = z_2 - \beta_1 e + \tau + \hat{C}^T(q,\dot{q})\dot{q} - \hat{G}(q) \\ \dot{z}_2 = -\beta_2 e \\ e = z_1 - y \end{cases} \tag{3.10}$$

where β_1 and β_2 are gain matrices of the observer, and

$$\begin{cases} z_1 = \hat{p} \\ z_2 = \hat{\tau}_{ext} \end{cases} \tag{3.11}$$

From (3.10), we can derive the transfer function, in the Laplace domain, from the input signal and momentum estimation as follows

$$\begin{cases} z_1 = \frac{z_2+\tau+\hat{C}^T(q,\dot{q})\dot{q}-\hat{G}(q)-\beta_1 p}{s+\beta_1} \\ z_2 = \frac{\beta_2 sp-\beta_2(\tau+\hat{C}^T(q,\dot{q})\dot{q}-\hat{G}(q))}{s^2+\beta_1 s+\beta_2} \end{cases} \tag{3.12}$$

Based on (3.12), the collision algorithm exhibits the characteristics of a critically damped second-order system. It comprises two adjustable parameters that represent key features of the dynamic system

$$\begin{cases} \omega_0 = \sqrt{\beta_2} \\ \zeta = \frac{\beta_1}{2\sqrt{\beta_2}} \end{cases} \tag{3.13}$$

where ω_0 is the bandwidth of the observer and ζ represents the damping ratio.

Using the parameters mentioned above in the extended state generalized momentum observer (ESGMO), the estimation error can swiftly converge from an initial non-zero value to zero, all without any oscillations. Furthermore, by appropriately tuning ω_0, we can achieve superior transient performance. However, it is important to note that in the case of an observer designed with a critically damping ratio, the external force detection may unavoidably exhibit peak value in the initial time (overshoots). Subsequently, to eliminate the overshoot, we have the option to augment the damping ratio during the initial phase. It is worth noting that the system's overshoot and accurate steady-state exhibit contrasting demands when it comes to the damping ratio. It is therefore necessary to find a compromise solution.

3.3. Composite observer strategy

A composite observer is based on the hybridization of the momentum observer and an extended state observer involves combining their respective features and functionalities to create a single observer that benefits from the strengths of both. In this study, our focus lies on the concept of switching hybridization. This approach entails the utilization of a switching logic mechanism to seamlessly transition between various observers in response to specific conditions, system states, or performance metrics. The underlying goal of this strategy is to facilitate adaptation to dynamic conditions and enhance estimation optimization.

The hybridization strategy that is described involves a two-phase approach using the EGSMO and the first-order momentum observer. Here is a summary of this hybridization strategy:

Phase 1: Extended State Generalized Momentum Observer (ESGMO) for Peak Elimination

Initial Time: During the initial phase or specific transient conditions where peak phenomena are likely to occur, the control system activates the ESGMO.

Peak Elimination: The primary role of the ESGMO in this phase is to eliminate or mitigate peak phenomena in the system's response. ESGMO excels in the estimation and can help smooth out the control signal to prevent overshoots or oscillations.

Transient Phase: ESGMO operates during the transient phase, ensuring that the system reaches a stable state without experiencing undesirable peaks in its response.

Phase 2: Generalized Momentum Observer (GMO) for Steady-State Accuracy

Switching to first-order momentum observer: Once the transient phase is complete, and the system has stabilized, the control system switches from ESGMO to the First-Order GMO.

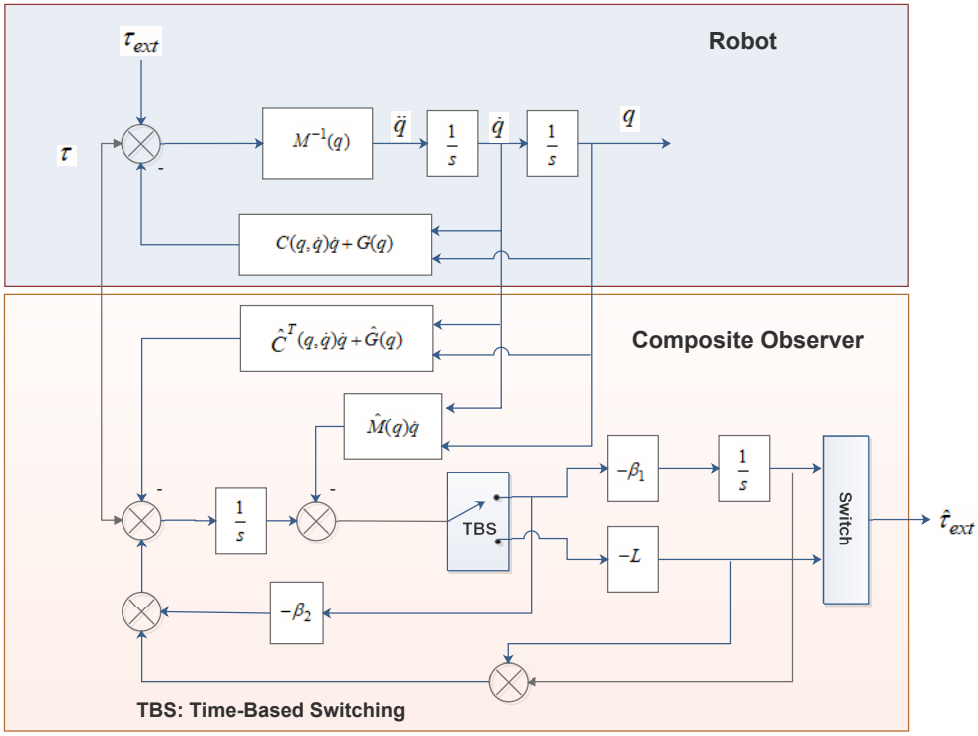

Figure 1. Block diagram of the composite observer.

Accuracy in Steady State: The First-Order Momentum Observer is employed in the steady-state phase to achieve accurate and precise control. It excels at providing stable and accurate control when the system is operating in a consistent manner.

Based on (3.5) and (3.10), the output of the composite observer can be defined as

$$\hat{\tau}_{ext} = \begin{cases} r_1, & t < Threshold \\ r_2, & t \geqslant Threshold \end{cases} \tag{3.14}$$

where

$$r_1 = L(p(t) - \int_0^t (\tau + \hat{C}^T(q,\dot{q})\dot{q} - \hat{G}(q) + \hat{\tau}_{ext})dv + p(0)) \tag{3.15}$$

and

$$r_2 = \beta_2(p(t) - \int_0^t (\hat{\tau}_{ext} - \beta_1(\hat{\tau}_{ext} - p) + \tau + \hat{C}^T(q,\dot{q})\dot{q} - \hat{G}(q))dv + p(0)) \tag{3.16}$$

In Figure 1, you can observe the block diagram representing the composite observer. During the initial phase, the monitoring signal $\hat{\tau}_{ext}$ consists of the residual vector derived from the extended state observer (ESO), denoted as z_2. However, in the steady-state condition, $\hat{\tau}_{ext}$ is comprised of the residual vector originating from the first-order momentum observer, which we label as r.

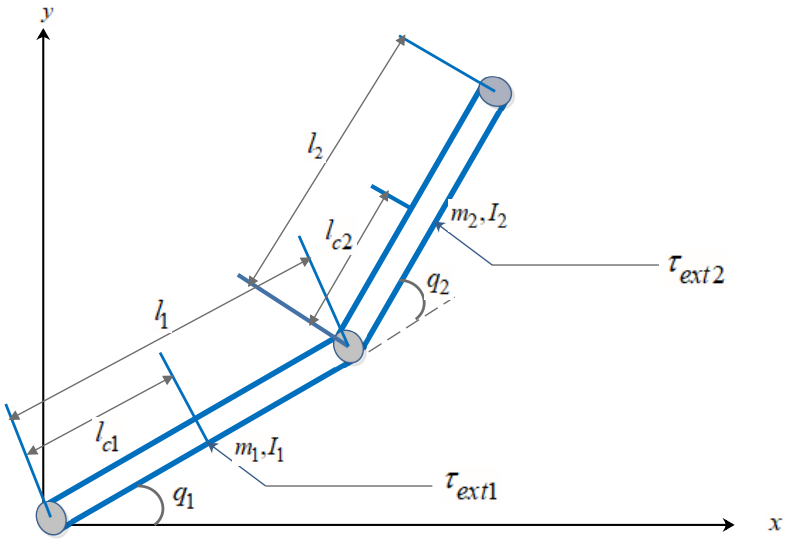

Figure 2. A 2-DOF robot architecture.

3.4. Convergence error observer

Within the collision detection algorithm, it is imperative that the observation error remains bounded under all circumstances. The proposed algorithm adopts the standard ESO structure from the active disturbance rejection control (ADRC) scheme, thus ensuring its stability and convergence properties. To delve into the error dynamics of ESO, we perform this analysis without any loss of generality.
The error of the observer can be obtained through (3.9) and (3.10) as

$$\begin{cases} \dot{e}_1 = e_2 - \beta_1 e_1 \\ \dot{e}_2 = -\beta_2 e_1 - \phi(t) \end{cases} \tag{3.17}$$

which can be rewritten as

$$\dot{E} = AE + B(-\phi(t)) \tag{3.18}$$

where

$$A = \begin{bmatrix} -\beta_1 & 1 \\ -\beta_2 & 0 \end{bmatrix} \text{ and } B = \begin{bmatrix} 0 \\ 1 \end{bmatrix}$$

such that β_1 and β_2 are calculated using the pole placement method. The desired reference signals are given as

$$q_{d1} = q_{d2} = sin(5t) \tag{3.19}$$

Assumption 1. *τ_{ext} is bounded, and thus $|\tau_{ext}| < \delta$, where δ is an unknown bounded value.*

Assumption 2. *$\phi(t)$ is an unknown bounded function $|\phi(t)| < \epsilon$, for a constant ϵ.*

We consider V the Lyapunov function of the dynamic error (3.18) as following

$$V = E^T S E \tag{3.20}$$

where S is a positive definite matrix, which satisfies

$$A^T S + S A = -\lambda I \tag{3.21}$$

$$\dot{V} = E^T (A^T S + S A) E + 2E^T S B(-\phi(t)) \tag{3.22}$$

Thus

$$\begin{aligned} \dot{V} &\leq -\lambda \|E\|^2 + 2\epsilon \lambda_{max}(S)\|E\| \\ &\leq -\|E\|(\lambda \|E\| - 2\epsilon \lambda_{max}(S)) \end{aligned} \tag{3.23}$$

where λ is positive and λ_{max} is the maximum eigenvalue of S. Given that the above assumptions are met, then E ultimately converges into the $\|E\| \leq \frac{2\epsilon \lambda_{max}(S)}{\lambda}$ bounded ball.

4. Simulation results

In order to examine the proposed method of collision detection and external force estimation, a 2-DOF planar robot is considered (Figure 2). The dynamic model takes the form

$$\begin{bmatrix} m_{11}(q) & m_{12}(q) \\ m_{21}(q) & m_{22}(q) \end{bmatrix} \begin{bmatrix} \ddot{q}_1 \\ \ddot{q}_1 \end{bmatrix} + \begin{bmatrix} c_1(d, \dot{q}) \\ c_2(d, \dot{q}) \end{bmatrix} + \begin{bmatrix} g_1(d) \\ g_2(d) \end{bmatrix} = \begin{bmatrix} \tau_1 \\ \tau_2 \end{bmatrix} + \begin{bmatrix} \tau_{d1} \\ \tau_{d2} \end{bmatrix} \tag{4.1}$$

where

$$\begin{cases} m_{11}(q) = m_1 l_{c1}^2 + m_2(l_1^2 + l_{c1}^2) + 2m_2 l_1 l_{c2} cos(q_2) + I_1 + I_2 \\ m_{12}(q) = m_{21}(q) = m_2 l_{c2}^2 + m_2 l_1 l_{c2} cos(q_2) + I_2 \\ m_{22}(q) = m_2 l_{c2}^2 + I_2 \\ c_1(q, \dot{q}) = -2m_2 l_1 l_{c2} \dot{q}_1 \dot{q}_1 sin(q_2) - m_2 l_1 l_{c2} \dot{q}_2^2 sin(q_2) \\ c_2(q, \dot{q}) = m_2 l_1 l_{c2} \dot{q}_1^2 sin(q_2) \\ g_1(q) = m_1 l_{c1} g cos(q_1) + m_2 g[l_{c2} cos(q_1 + q_2) + l_1 cos(q_1)] \\ g_2(q) = m_2 g l_{c2} cos(q_1 + q_2) \end{cases} \tag{4.2}$$

and
$m_1 = 1$ kg, $m_2 = 0.8$ kg, $l_1 = 0.5$ m, ł$_2 = 0.25$ m, $l_{c1} = 0.25$ m, $l_{c2} = 0.125$ m, $I_1 = 1$ kg.m^2, $I_2 = 0.8$ kg.m^2 and $g = 9.8$ m/s^2

We will adopt the computed torque control strategy, which, without imposing any loss of generality, can effectively fulfill the fixed-point control demands of the robot manipulator. The composite observer-based approach described above is employed for the estimation of external forces applied on the manipulator, and a comparison between this observer and others is conducted.

The first case of simulation shows the limitations of the momentum observer and the extended state observer such as the influence of the observer parameters on the estimation sensitivity and the peak value, while the second case shows the performance of the composite observer and a comparison between it and previous observers.

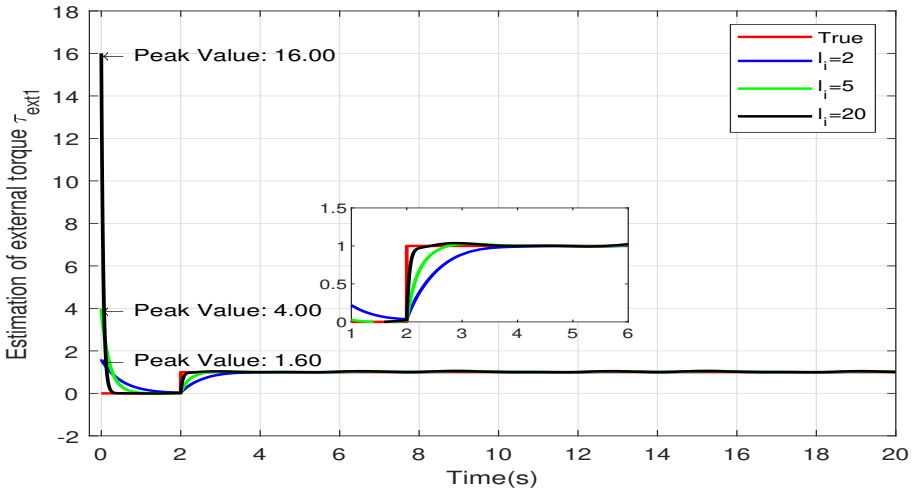

(a) First link

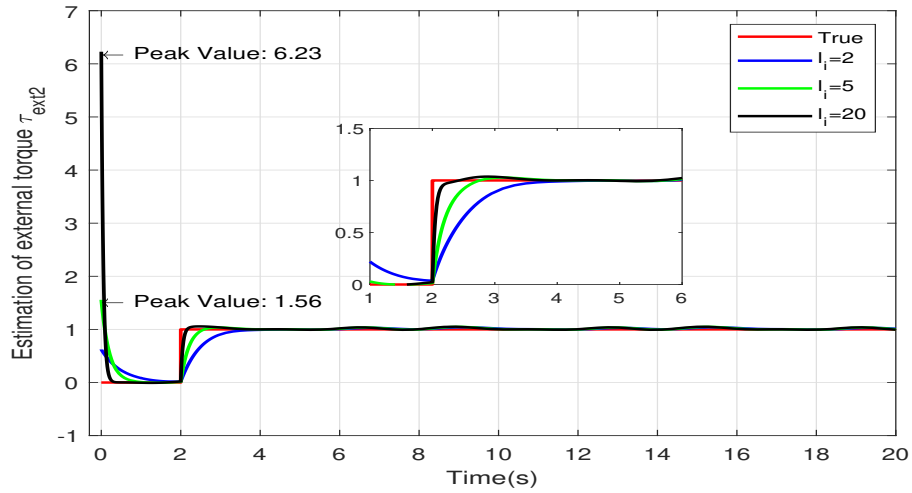

(b) Second link

Figure 3. External torque estimation using GMO.

4.1. Case 1

The observer gain influences the performance of the observer in several ways, and it can have a significant impact on the residual of the observer. The residual is the difference between the actual measurements and the estimate measurements by the observer. In this case, each observer is used to illustrate the impact of its parameters on the residual value, and the external torques resulting from collision are defined as

$$\tau_{ext1} = \tau_{ext2} = \begin{cases} 0, & t < 2 \\ 1, & t \geqslant 2 \end{cases} \tag{4.3}$$

From Figure 3, the gain of the generalized momentum observer L affects the convergence rate of the observer. Higher gains can lead to faster convergence, meaning that the estimated states converge to the actual states more quickly. However, excessively high gains may introduce an important peak.

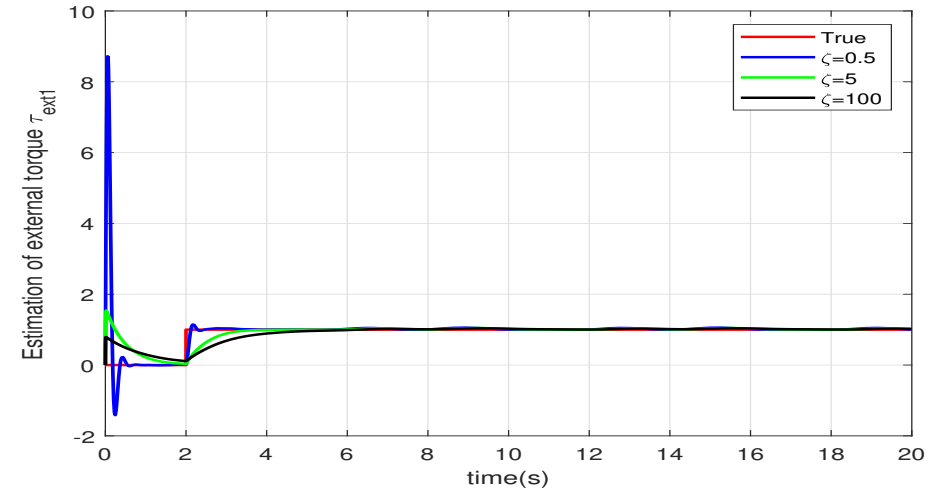

(a) First link

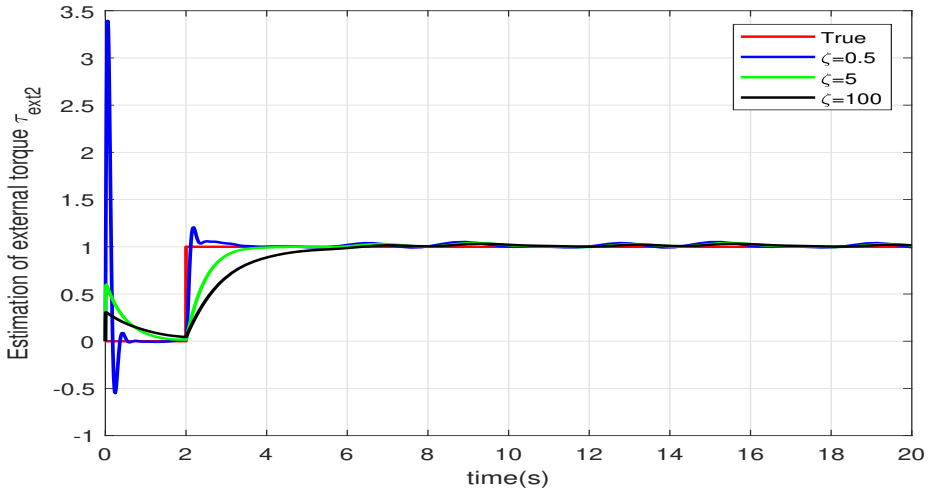

(b) Second link

Figure 4. External torque estimation using ESGMO.

While the estimation of external torque using an extended state observer in Figure 4, from Eq (3.13), it is evident that altering the damping ratio ζ inevitably results in a forced change in bandwidth ω_0. Detecting external forces by the observer with a critically damping ratio will inevitably lead to overshoots. Increasing the damping ratio at the initial time allows us to eliminate the peak value. However, it becomes evident that the system's overshoot and steady-state error demand contrasting damping ratio values. Therefore, a compromise solution becomes necessary.

4.2. Case 2

Commencing with the identified limitations of both the generalized momentum observer (GMO) and extended state generalized momentum observer (ESGMO), we initiated the estimation process by employing the extended observer in the initial phase, incorporating a significant damping ratio to

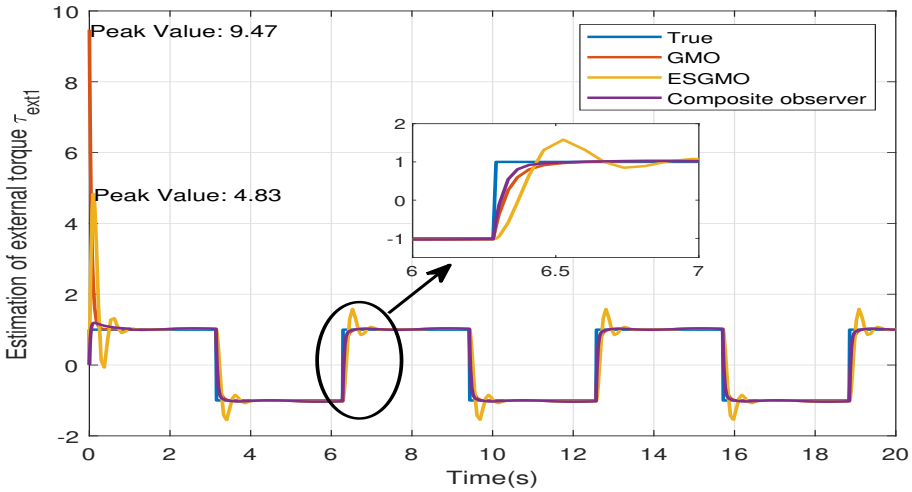

(a) First link

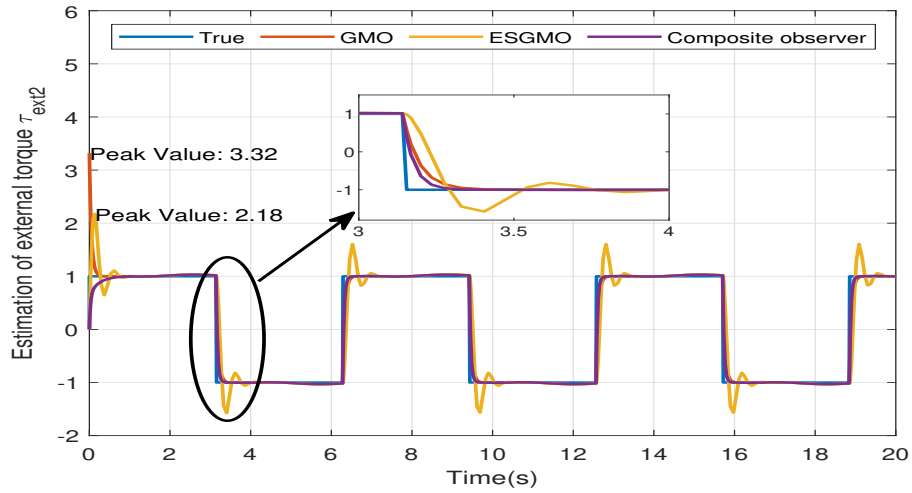

(b) Second link

Figure 5. Estimation of the external torque with three observers.

mitigate the occurrence of peak phenomena. Subsequently, as time progresses beyond the initial phase, we transition to a generalized momentum observer, leveraging its assured gain to enhance tracking accuracy. Table 1 describes the parameters setting of the composite observer.

We assume that the collision force can be translated as a square function:

$$\tau_{ext1} = \tau_{ext2} = sign(sin(5t)) \tag{4.4}$$

The peak value of external torque varies among joints, as indicated by the estimated results, and this discrepancy can be attributed to the mass of each respective joint. As illustrated in Figure 5, the torque estimated using GMO, the peak value for the first joint is 9.47 and for the second joint is 3.32. This variation is attributed to the respective masses of the robot's joints, with the first and second joints weighing 1 kg and 0.8 kg, respectively. Therefore, the dynamics of the observer's gain, leading to the occurrence of the peak phenomenon, are influenced by the mass of the joint.

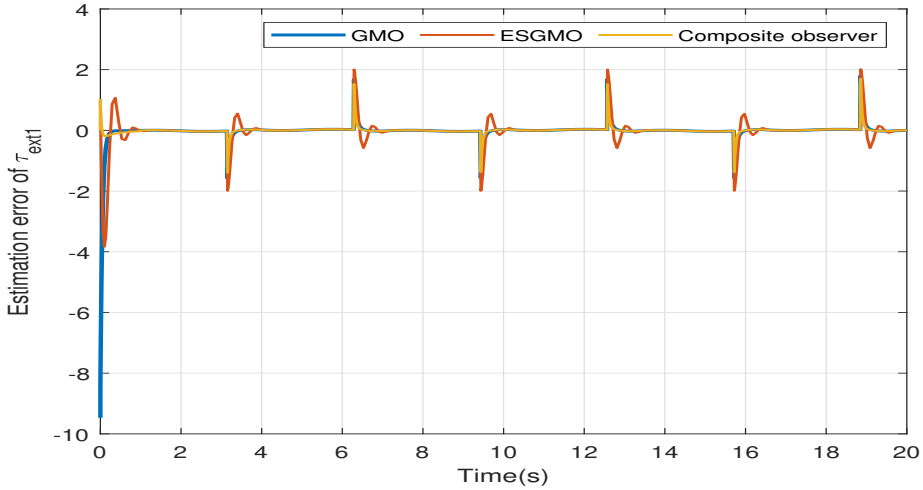

(a) First link

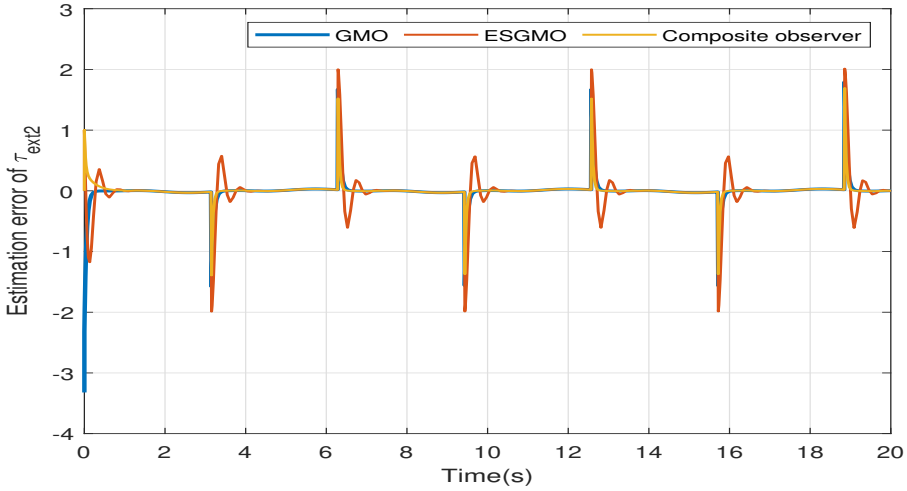

(b) Second link

Figure 6. Estimation error of the external torque.

As discussed in the introduction, the goal of this study is to minimize the peak value while preserving the sensitivity of collision estimation, as depicted in the figures. Both GMO and ESGMO observers exhibit a noticeable peak, unlike the composite observer, which nearly eradicates the peak entirely. The Figure 6 also illustrates that the composite observer exhibits a lower peak value compared to GMO and ESGMO. This can be attributed to its damping ratio ζ in the initial time. When the torque estimation error is non-zero, the composite observer strives to rapidly converge to zero, contingent on the definition of an appropriate gain, denoted as L.

Figure 7 illustrates the $\mathcal{L}_2$-performance index. It is evident that the composite observer outperforms others due to its tuning, enabling enhanced convergence rates. Furthermore, the mean absolute error (MAE) and the mean square error (MSE) performance indexes are integral to our comparative analysis. Table 2 clearly demonstrates that our proposed observer significantly enhances accuracy in comparison to GMO and ESGMO methods.

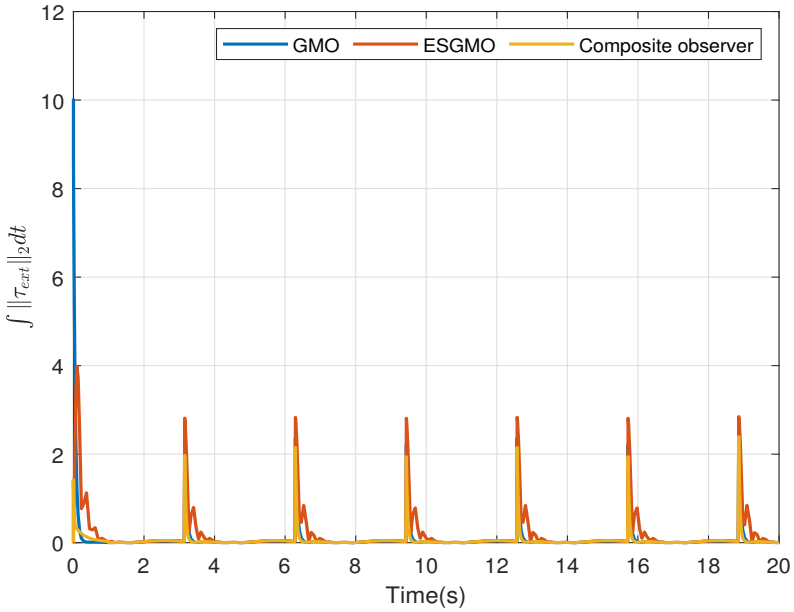

Figure 7. $\mathcal{L}_2$-performance index.

Table 1. Parameters setting of the composite observer.

ESGMO	$\beta_1 = \begin{pmatrix} 40 & 0 \\ 0 & 40 \end{pmatrix}, \beta_2 = \begin{pmatrix} 100 & 0 \\ 0 & 150 \end{pmatrix}$
Time transition	2s
GMO	$L = \begin{pmatrix} 30 & 0 \\ 0 & 30 \end{pmatrix}$

Table 2. Comparison of observers' performance (MAE & MSE).

	1^{st} joint		2^{nd} joint	
	MAE	MSE	MAE	MSE
GMO	0.36	0.17	2.08	0.27
ESGMO	0.28	0.23	0.47	0.29
Composite observer	0.11	0.10	0.09	0.09

5. Conclusions

Among the collision detection methods, there is a general consensus that the momentum dynamic-based method is the most accurate, reliable, and cost-effective. In this paper, an alternative method based on momentum dynamics was presented for collision detection and estimation of external forces for robot manipulators. To improve detection accuracy and estimation performance, a hybrid momentum observer was designed, which was composed of a first-order generalized momentum observer and an extended state observer. The collision detection system worked in the initial time using ESGMO with a suitable bandwidth to eliminate peak phenomena and avoid false alarm, and

once the peak moment had passed, the collision detection system switched to the momentum observer with appropriate gain to achieved high sensitivity in force estimation. Through their complementary roles, the composite observer achieved improved performance in terms of sensitivity and reducing the peaking value. This algorithm was used for the detection of collisions but should be enhanced to trigger an appropriate reaction for the robot arms when the event occurs. The proposed method can be applied to all types of manipulator arms, as we have utilized the model of an n-degree-of-freedom robot manipulator. In this study, we tested this method on a 2-DOF arm to examine and explain its effectiveness. Nonetheless, it is also applicable to other types of arms. In future work, this approach will be incorporated on a real platform for industrial applications such as welding and painting. Additionally, we plan to propose a 6-degree-of-freedom model and validate it experimentally.

Author contributions

Benaoumeur Ibari: Conceptualization, Software, Validation, Investigation, Resources, Writing – review & editing, Writing-original draft, Methodology, Supervision, Formal Analysis; Mourad Hebali: Writing-original draft, Software, Validation, Formal analysis, Investigation, Project administration, Data curation, Visualization; Baghdadi Rezali: Formal Analysis, Writing-original draft, Investigation, Project administration, Data curation, Visualization, Writing – review & editing, Supervision; Menaouer Bennaoum: Software, Validation, Investigation, Visualization, Writing – review & editing, Resources, Supervision. All authors have read and approved the final version of the manuscript for publication.

Use of AI tools declaration

The authors declare they have not used Artificial Intelligence (AI) tools in the creation of this article.

Conflict of interest

The authors declare that there are no conflicts of interest in this paper.

References

1. Haninger K, Radke M, Vick A, Krüger J (2022) Towards high-payload admittance control for manual guidance with environmental contact. *IEEE Robot Autom Lett* 7: 4275–4282. https://doi.org/10.1109/LRA.2022.3150051
2. Villani V, Pini F, Leali F, Secchi C (2018) Survey on human–robot collaboration in industrial settings: Safety, intuitive interfaces and applications. *Mechatronics* 55: 248–266. https://doi.org/10.1016/j.mechatronics.2018.02.009
3. Vicentini F (2021) Collaborative robotics: a survey. *J Mech Design* 143: 040802. https://doi.org/10.1115/1.4046238
4. Ferraguti F, Landi CT, Singletary A, Lin HC, Ames A, Secchi C, et al. (2022) Safety and efficiency in robotics: The control barrier functions approach. *IEEE Robot Autom Mag* 29: 139–151. https://doi.org/10.1109/mra.2022.3174699

5. Cirillo A, Ficuciello F, Natale C, Pirozzi S, Villani L (2015) A conformable force/tactile skin for physical human–robot interaction. *IEEE Robot Autom Lett* 1: 41–48. https://doi.org/10.1109/LRA.2015.2505061

6. Pang G, Yang G, Heng W, Ye Z, Huang X, Yang H, et al. (2020) CoboSkin: Soft robot skin with variable stiffness for safer human–robot collaboration. *IEEE T Ind Electron* 68: 3303–3314. https://doi.org/10.1109/TIE.2020.2978728

7. Hughes D, Lammie J, Correll N (2018) A robotic skin for collision avoidance and affective touch recognition. *IEEE Robot Autom Lett* 3: 1386–1393. https://doi.org/10.1109/LRA.2018.2799743

8. Ye Z, Pang G, Xu K, Hou Z, Lv H, Shen Y, et al. (2022) Soft robot skin with conformal adaptability for on-body tactile perception of collaborative robots. *IEEE Robot Autom Lett* 7: 5127–5134. https://doi.org/10.1109/LRA.2022.3155225

9. Flacco F, Kröger T, De Luca A, Khatib O (2012) A depth space approach to human-robot collision avoidance. *2012 IEEE International Conference On Robotics And Automation* 338–345. https://doi.org/10.1109/ICRA.2012.6225245

10. Wisanuvej P, Liu J, Chen C, Yang G (2014) Blind collision detection and obstacle characterisation using a compliant robotic arm. *2014 IEEE International Conference On Robotics And Automation (ICRA)* 2249–2254. https://doi.org/10.1109/ICRA.2014.6907170

11. Sandykbayeva D, Kappassov Z, Orazbayev B (2022) Vibrotouch: Active tactile sensor for contact detection and force sensing via vibrations. *Sensors* 22: 6456. https://doi.org/10.3390/s22176456

12. Katsampiris-Salgado K, Haninger K, Gkrizis C, Dimitropoulos N, Krüger J, Michalos G, et al. (2024) Collision detection for collaborative assembly operations on high-payload robots. *Robot Com-Int Manuf* 87: 102708. https://doi.org/10.1016/j.rcim.2023.102708

13. Sharkawy A, Koustoumpardis P, Aspragathos N (2019) Manipulator collision detection and collided link identification based on neural networks. *Advances In Service And Industrial Robotics: Proceedings Of The 27th International Conference On Robotics In Alpe-Adria Danube Region (RAAD 2018)* 3–12. https://doi.org/10.1007/978-3-030-00232-9_1

14. Min F, Wang G, Liu N (2019) Collision detection and identification on robot manipulators based on vibration analysis. *Sensors* 19: 1080. https://doi.org/10.3390/s19051080

15. Heo Y, Kim D, Lee W, Kim H, Park J, Chung W (2019) Collision detection for industrial collaborative robots: A deep learning approach. *IEEE Robot Autom Lett* 4: 740–746. https://doi.org/10.1109/LRA.2019.2893400

16. Narukawa K, Yoshiike T, Tanaka K, Kuroda M (2017) Real-time collision detection based on one class SVM for safe movement of humanoid robot. *2017 IEEE-RAS 17th International Conference On Humanoid Robotics (Humanoids)* 791–796. https://doi.org/10.1109/HUMANOIDS.2017.8246962

17. Dimeas F, Avendaño-Valencia L, Aspragathos N (2015) Human-robot collision detection and identification based on fuzzy and time series modelling. *Robotica* 33: 1886–1898. https://doi.org/10.1017/S0263574714001143

18. Jing X, Guangxin W, Chongyang L, Hong L (2016) Real-time collision detection for manipulators

based on fuzzy synthetic evaluation. *2016 IEEE International Conference On Mechatronics And Automation* 777–782. https://doi.org/10.1109/ICMA.2016.7558661

19. Sedigh Ziyabari H, Aliyari Shoorehdeli M (2018) Fuzzy robust fault estimation scheme for a class of nonlinear systems based on an unknown input sliding mode observer. *J Vib Control* 24: 1861–1873. https://doi.org/10.1177/1077546316669
20. Caccavale F, Walker I (1997) Observer-based fault detection for robot manipulators. *Proceedings Of International Conference On Robotics And Automation* 4: 2881–2887. https://doi.org/10.1109/ROBOT.1997.606724
21. Morinaga S, Kosuge K (2003) Collision detection system for manipulator based on adaptive impedance control law. *2003 IEEE International Conference On Robotics And Automation (Cat. No. 03CH37422)* 1: 1080–1085. https://doi.org/10.1109/ROBOT.2003.1241736
22. Haddadin S (2013) *Towards safe robots: Approaching Asimov's 1st law.* , Springer Tracts in Advanced Robotics, Vol. 90, Berlin, Heidelberg Springer. https://doi.org/10.1007/978-3-642-40308-8
23. Hu J, Xiong R (2017) Contact force estimation for robot manipulator using semiparametric model and disturbance Kalman filter. *IEEE T Ind Electron* 65: 3365–3375. https://doi.org/10.1109/TIE.2017.2748056
24. De Luca A, Mattone R (2003) Actuator failure detection and isolation using generalized momenta. *2003 IEEE International Conference On Robotics And Automation (cat. No. 03CH37422)* 1: 634–639. https://doi.org/10.1109/ROBOT.2003.1241665
25. Haddadin S, De Luca A, Albu-Schäffer A (2017) Robot collisions: A survey on detection, isolation, and identification. *IEEE T Robot* 33: 1292–1312. https://doi.org/10.1109/TRO.2017.2723903
26. Garofalo G, Mansfeld N, Jankowski J, Ott C (2019) Sliding mode momentum observers for estimation of external torques and joint acceleration. *2019 International Conference On Robotics And Automation (ICRA)* 6117–6123. https://doi.org/10.1109/ICRA.2019.8793529
27. Long S, Dang X, Sun S, Wang Y, Gui M (2022) A Novel Sliding Mode Momentum Observer for Collaborative Robot Collision Detection. *Machines* 10: 818. https://doi.org/10.3390/machines10090818
28. Zhang C, Mu C, Wang Y, Li J, Liu Z (2023) Collision detection for six-DOF serial robots force/position hybrid control based on continuous friction model. *Measurement and Control* 56: 571–582. https://doi.org/10.1177/00202940221091575
29. Abdelaziz O, Luo M, Jiang G, Chen S (2020) Adaptive threshold for robot manipulator collision detection using fuzzy system. *SN Appl Sci* 2: 319. https://doi.org/10.1007/s42452-020-2110-z
30. Birjandi S, Kühn J, Haddadin S (2020) Observer-extended direct method for collision monitoring in robot manipulators using proprioception and IMU sensing. *IEEE Robot Autom Lett* 5: 954–961. 10.1109/LRA.2020.2967287
31. Ren T, Dong Y, Wu D, Chen K (2018) Collision detection and identification for robot manipulators based on extended state observer. *Control Eng Pract* 79: 44–153. https://doi.org/10.1016/j.conengprac.2018.07.004

32. Li Y, Li Y, Zhu M, Xu Z, Mu D (2021) A nonlinear momentum observer for sensorless robot collision detection under model uncertainties. *Mechatronics* 78: 102603. https://doi.org/10.1016/j.mechatronics.2021.102603

33. Murray R, Li Z, Sastry S, Sastry S (1994) *A mathematical introduction to robotic manipulation*, 1st Eds., California, Boca Raton: CRC press, 519. https://doi.org/10.1201/9781315136370

34. De Luca A, Mattone R (2005) Sensorless robot collision detection and hybrid force/motion control. *Proceedings Of The 2005 IEEE International Conference On Robotics And Automation* 999–1004. https://doi.org/10.1109/ROBOT.2005.1570247

35. De Luca A, Albu-Schaffer A, Haddadin S, Hirzinger G (2006) Collision detection and safe reaction with the DLR-III lightweight manipulator arm. *2006 IEEE/RSJ International Conference On Intelligent Robots And Systems* 1623–1630. https://doi.org/10.1109/IROS.2006.282053

36. Han J (2009) From PID to active disturbance rejection control. *IEEE T Ind Electron* 56: 900–906. https://doi.org/10.1109/TIE.2008.2011621

AIMS Press